*Carbohydrate Research*, 214 (1991) 299–314
Elsevier Science Publishers B.V., Amsterdam



# Structure and solution properties of tamarind-seed polysaccharide

Michael J. Gidley*, Peter J. Lillford, David W. Rowlands,
*Unilever Research Laboratory, Colworth House, Sharnbrook, Bedford MK44 1LQ (Great Britain)*

Peter Lang, Mariella Dentini, Vittorio Crescenzi,
*Dipartimento di Chimica, Universita di Roma "La Sapienza", I-00185 Roma (Italy)*

Mary Edwards, Cristina Fanutti, and J. S. Grant Reid
*School of Molecular and Biological Sciences, University of Stirling, Stirling FK9 4LA (Great Britain)*

(Received July 9th, 1990; accepted for publication, October 24th, 1990)

ABSTRACT

The major polysaccharide in tamarind seed is a galactoxyloglucan for which the ratios galactose:xylose:glucose are 1:2.25:2.8. A minor polysaccharide (2–3%) contains branched (1→5)-α-L-arabinofuranan and unbranched (1→4)-β-D-galactopyranan features. Small-angle X-ray scattering experiments gave values for the cross-sectional radius of the polymer in aqueous solution that were typical of single-stranded molecules. Marked stiffness of the chain ($C_\infty$ 110) was deduced from static light-scattering studies and is ascribed partially to the restriction of the motion of the (1→4)-β-D-glucan backbone by its extensive (~80%) glycosylation. The rigidity of the polymer caused significant draining effects, which heavily influenced the hydrodynamic behaviour. The dependence of "zero-shear" viscosity on concentration was used to characterise "dilute" and "semi-dilute" concentration regimes. The marked dependence on concentration in the "semi-dilute" region was similar to that for other stiff neutral polysaccharide systems, ascribed to "hyperentanglements", and it is suggested that these may have arisen through a tenuous alignment of stiffened chains.

## INTRODUCTION

Seeds of the tamarind tree (*Tamarindus indica*), which is indigenous to India and South East Asia, contain large proportions of a non-starch polysaccharide that functions as an energy reserve[1,2]. Seeds are present in pods, which also contain a pulp that is widely used in Asian cuisine and has high concentrations of sugars and tartaric acid[3]. As tamarind seeds are a by-product of the extraction of pulp, commercial applications have been sought. De-hulled and crushed seeds provide a crude preparation of polysaccharide (tamarind-kernel powder) which is used, for example, in textile sizing and weaving, and as an adhesive or binding agent in other industries[4]. A soluble (tamarind-seed) polysaccharide fraction can be prepared from the powder of the kernel and is used as a thickening, stabilising, and gelling agent in foods, particularly in Japan where it is a permitted food additive[5].

* Author for correspondence.

0008-6215/91/$03.50 

Tamarind-seed polysaccharide belongs to the xyloglucan family, members of which are found either within the cell-wall matrices of plants[6] or as major seed components and, presumably, function as energy reserves[1,7]. Xyloglucans are often termed "amyloids" because of the characteristic blue stain that is produced with iodine/potassium iodide solution[7]. Although all seed "xyloglucans" examined to date have common structural elements (**1**), *i.e.*, a cellulosic-type (1→4)-β-D-glucan backbone with side chains of α-D-xylopyranose and β-D-galactopyranosyl-(1→2)-α-D-xylopyranose (1→6)-linked to the backbone, two features of the structure are not well defined. Firstly, the ratios of glucose:xylose:galactose, often reported[1,4,5] as ~3:2:1, have been determined variously to be 3:2.25:1 (ref. 8), 2.25:1.25:1 (ref. 9), 3:2:1 (refs. 10–12), and 4:2:1 (ref. 13). Secondly, the presence of low proportions of arabinose residues has been reported[9,11,13] in acid hydrolysates of preparations of tamarind-seed polysaccharide. It has been suggested[13] that arabinofuranosyl residues are (1→2)-linked to the cellulosic backbone, but there is no conclusive evidence. Two other possibilities, which have not been considered previously, are that arabinose may be present due to a contaminating arabinan or that α-L-arabinofuranose may be (1→6)-linked to side-chain xylose residues as is found in tobacco cell walls[14]. This latter possibility gains credence from the similarity in structure of α-L-arabinose and β-D-galactose, which is (1→2)-linked to xylose in tamarind-seed polysaccharide (**1**). α-Arabinofuranose is (1→2)-linked to a specific xylose-substituted glucose residue in a minor oligosaccharide obtained[15] by enzymic degradation of the extracellular xyloglucan from sycamore.

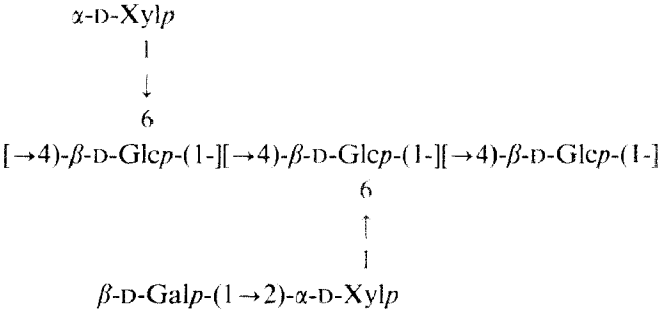


**1**

Commercial interest in purified tamarind-seed polysaccharide centres on its ability to thicken or gel aqueous-based food systems[5]. In aqueous solution, tamarind-seed polysaccharide is an effective viscosifier[5], whereas gels are formed in the presence of ~50% of sugar (or alcohols). Despite these applications, there have been few detailed studies of the molecular properties of solutions of tamarind-seed polysaccharide or other xyloglucans. From a consideration of the structure (**1**), the cellulosic backbone with a high degree of glycosyl substitution would be expected[16] to lead to a stiff, extended-chain structure in solution and, hence, efficient volume occupancy and enhancement of viscosity. Light-scattering studies[17–19] of another glycosyl-branched cellulosic polysaccharide, xanthan, have revealed an extremely stiff molecular structure, at

least in the "ordered" conformation. The rheological properties of xanthan[20] are typical of "weak gels" rather than of simple (entanglement) solutions, such as shown by guar gum[21], another branched polysaccharide with a moderately stiff backbone. Therefore, it is of interest to characterise the behaviour in solution of tamarind-seed polysaccharide, both in terms of the chain dimensions and persistence of the chains as well as macroscopic rheological behaviour.

We now report on the structure and properties in aqueous solution of tamarind-seed polysaccharide.

## RESULTS AND DISCUSSION

*Composition.* — Tamarind-seed polysaccharides from various commercial sources were purified and their compositions, determined by acid hydrolysis and g.l.c. of the derived alditol acetates, were glucose, 43–45%; xylose, 35–38%; galactose, 15–17%; and arabinose, 2–3%. Similar results were obtained for the polysaccharide from nasturtium seed.

The composition was investigated also by $^1$H-n.m.r. spectroscopy. The spectrum of the region for signals of anomeric protons is shown in Fig. 1a. From analyses of related systems[14,22], the signals at 5.15 (d, $J_{1,2}$ 3.3 Hz), 4.97 (d, $J_{1,2}$ 3.4 Hz), and 4.55–4.65 p.p.m. were assigned to H-1 of 2-*O*-galactosylxylose, terminal xylose, and all of the glucose and galactose residues, respectively, in **1**. Other minor signals in the range

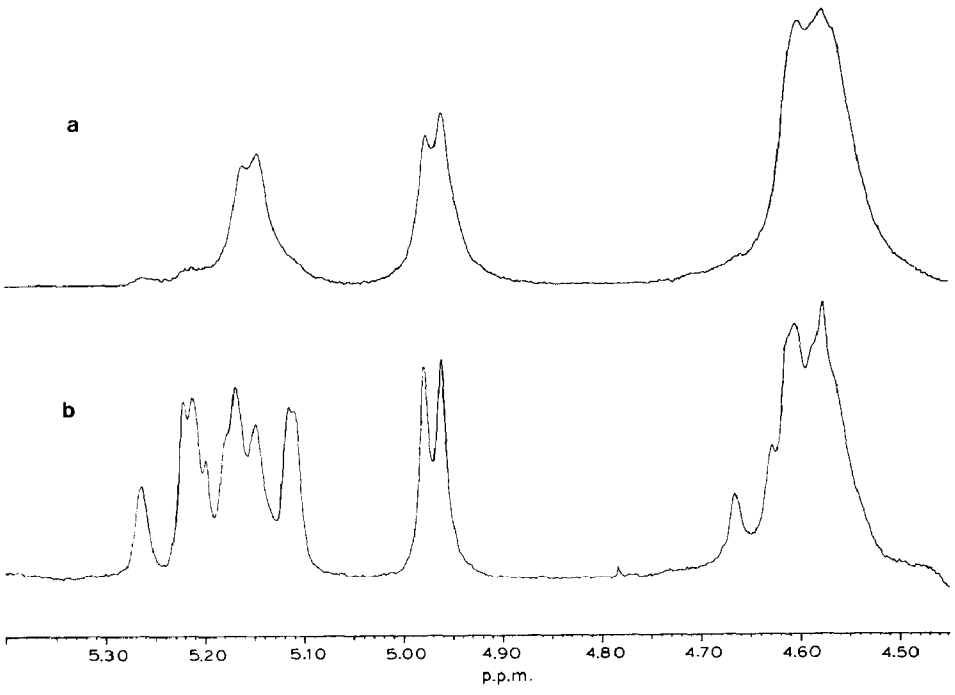


Fig. 1. Partial $^1$H-n.m.r. spectra (90°, 2 mg/mL in $D_2O$) of (*a*) tamarind-seed polysaccharide (purified Glyloid 3S) and (*b*) the fraction soluble in alkaline copper sulphate and enriched in arabinan.

5.1–5.3 p.p.m. are assigned to H-1 of arabinose residues (see below).

The ratios of the residues could be determined from the intensities of the appropriate signals for galactose (5.15 p.p.m.), xylose (sum of the signals at 5.15 and 4.97 p.p.m.), and glucose (difference between the signals at 4.55–4.65 and 5.15 p.p.m.). In order to obtain reliable quantitative data, it was necessary to allow for full relaxation of resonances between consecutive observation pulses; the $T_1$ values for the relevant $^1H$ resonances for native and depolymerised tamarind-seed polysaccharides are shown in Table I. The $T_1$ values for the resonances of H-1 of glucose and galactose were not sensitive to molecular weight, whereas those for the resonances of H-1 of the substituted and terminal xylose residues increased with decrease in the molecular weight. 2-*O*-Galactosyl substitution markedly lowered the $T_1$ value of the xylose H-1 resonance and those of the H-1 resonances of galactose and glucose were similar. Although there is no general relationship between the $T_1$ values for resonances of polysaccharides and local molecular mobilities, the results shown in Table I are consistent with hindered mobility about the β-galactosyl-(1→2)-xylose linkage as might be predicted on the basis of steric compression. For quantitative analysis of the composition, a delay of at least 5 s (*i.e.*, 5 times the longest $T_1$ value found for the resonances of the low-molecular-weight materials) was employed. $^1H$-N.m.r. analysis of several commercial tamarind-seed polysaccharides yielded residue compositions of glucose, 44–46%; xylose, 35–38%; galactose, 15–17%; and arabinose, 2–3%. Similar results were obtained for nasturtium-seed polysaccharide. These results are essentially identical to those noted above, which were obtained by g.l.c. of the alditol acetates, and confirmed that, for several preparations of tamarind-seed polysaccharide, the ratios glucose:xylose:galactose:arabinose are 45 ± 1:36 ± 1:16 ± 1:2–3. As shown below, the arabinose was probably due to a contaminating arabinan. The ratios for tamarind-seed galactoxyloglucan are therefore 2.80 (±0.05):2.25 (±0.05):1.0 for glucose:xylose:galactose. These ratios are significant-

TABLE I

$T_1$ values (s) for the H-1 resonances in tamarind-seed polysaccharide[a]

| *Signal* | *Native*[b] | *Depolymerised*[c] | |
|---|---|---|---|
| | $T_1$ | $T_1$ | |
| | | *D.p.* ~50[d] | *D.p.* ~10[e] |
| 2-*O*-Galactosylxylose (5.15 p.p.m.) | 0.52 | 0.58 | 0.66 |
| Terminal xylose (4.97 p.p.m.) | 0.67 | 0.85 | 1.0 |
| Glucose + galactose (4.55–4.65 p.p.m.) | 0.57–0.61 | 0.47–0.58 | 0.48–0.55 |

[a] In solution in $D_2O$ at 90°. [b] Purified Glyloid 3S. [c] Glyloid after treatment with xyloglucan-specific endo-β-D-glucanase from nasturtium[23]. [d] Total endo-β-D-glucanase digest; d.p. determined by quantitative $^1H$-n.m.r. analysis of the signals for anomeric protons. [e] After fractionation of endo-β-D-glucanase digest on Sephadex G-50 (fraction with greatest elution volume).

ly different from those (3:2:1) reported frequently and indicate a higher degree of backbone substitution than found previously, although the ratios are similar to those (3:2.25:1) reported by Kooiman[8].

*Features of the arabinan.* — Arabinose residues were found in the tamarind-seed polysaccharides studied here and elsewhere[9,11,13]. The $^1$H-n.m.r. spectrum (Fig. 1a) suggested that the H-1 resonances associated with the arabinose residues occurred at 5.1–5.3 p.p.m. An arabinose-related signal has been reported[14] at ~5.1 p.p.m. for an arabinoxyloglucan isolated from tobacco cell walls. In this molecule, L-arabinofuranose residues were 2-linked to some α-xylopyranosyl side-chains that were 6-linked to a (1→4)-β-D-glucan backbone[14]. In order to determine whether a similar structure occurs in tamarind-seed polysaccharide, $^{13}$C-n.m.r. spectra were recorded, because Mori *et al.*[14] have reported that the arabinosyl C-1 resonance in tobacco arabinoxyloglucan has a chemical shift of 111.2 p.p.m. The $^{13}$C-n.m.r. spectrum of tamarind-seed polysaccharide is shown in Fig. 2a, and the C-1 signals at 105.5, 103.4, and 100.1 p.p.m. were assigned to galactose, glucose, and xylose residues, respectively. Although there appeared to be several other signals of low intensity, the limited signal-to-noise ratio, achieved with the viscous 0.5% solution employed, rendered the identification of the minor signals ambiguous.

Following treatment of tamarind-seed polysaccharide with nasturtium endo-(1→4)-β-D-glucanase[23], the $^{13}$C-n.m.r. spectrum of an aqueous 3% solution shown in

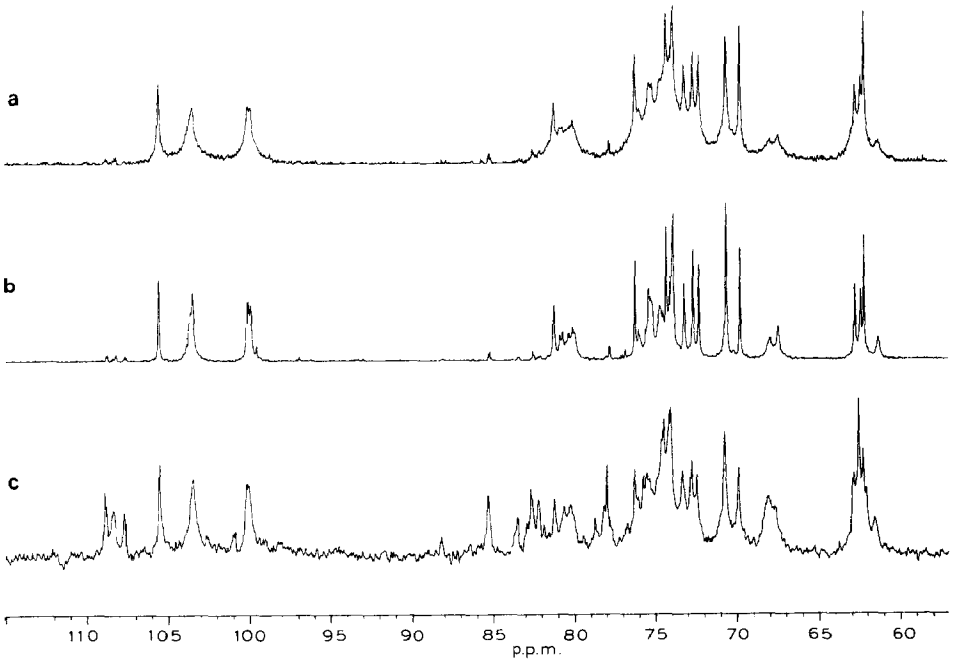


Fig. 2. $^{13}$C-N.m.r. spectra of (*a*) tamarind-seed polysaccharide (90°, 5 mg/mL in $D_2O$), (*b*) the same sample after digestion with nasturtium endo-(1→4)-β-D-glucanase[23] (60°, 30 mg/mL in $D_2O$), and (*c*) the fraction from (*a*) that was soluble in alkaline copper sulphate and enriched in arabinan.

Fig. 2b was recorded. Minor signals, characteristic of furanose structures, were present in the regions 75–86 and 107–109 p.p.m., and are ascribed to arabinose. The chemical shifts of the three most intense of the latter signals (108.67, 108.12, and 107.57 p.p.m.) were essentially identical to those (108.7, 108.15, and 107.6 p.p.m.) reported by Capek *et al.*[24] for an arabinan isolated from marsh mallow (*Althaea officinalis* L.). All other minor signals attributed to arabinose in the depolymerised tamarind-seed polysaccharide had chemical shifts that are essentially identical to those reported by Capek *et al.*[24] for a (1→5)-linked α-L-arabinofuranan backbone with side chains of (1→2)- and (1→3)-linked α-L-arabinofuranose. Similar chemical shift and structural data have been reported for an arabinan from *Rosa glauca*[25]. Although tentative assignments for these resonances have been proposed[14], no definitive $^{13}C$ assignments are available for branched arabinans. Chemical shifts for the H-1 resonances of the *R. glauca* arabinan were reported[25] to be in the range 5.0–5.4 p.p.m., in agreement with those of the minor signals given by the tamarind-seed polysaccharide (Fig. 1a). Similarly, Churms *et al.*[26] reported a chemical shift of 5.1 p.p.m. for the H-1 resonance of a linear (1→5)-linked α-L-arabinan. The low (unresolved) $J_{1,2}$ values for tamarind-seed polysaccharides are more consistent with those expected[27] for α-L-arabinofuranose residues (1.2–2.9 Hz) than for the β form (4.3–4.8 Hz).

The arabinan-like linkages observed in tamarind-seed polysaccharide may arise either through covalent attachment of arabinan side chains to the galactoxyloglucan core or through the co-purification of an arabinan. Depolymerisation of tamarind-seed polysaccharide with nasturtium endo-(1→4)-β-D-glucanase[23] gave a mixture of low-molecular-weight fragments that could be resolved partially by chromatography on Sephadex G-50 (data not shown). $^1H$-N.m.r. analysis of the fractions showed the absence of the characteristic arabinose H-1 signals in the range 5.0–5.4 p.p.m., except for the fraction of highest molecular weight (d.p. ~ 100 by end-group analysis based on $^1H$-n.m.r. data). This evidence suggests that arabinans are not present as short oligomeric side chains attached to the galactoxyloglucan core. Significant enrichment of the arabinan was obtained by precipitation of the tamarind-seed polysaccharide with alkaline copper sulphate. The material (2.3%) in the supernatant solution contained ~30% of arabinan and ~70% of galactoxyloglucan (Fig. 1b), the latter having essentially the same glucose:xylose:galactose ratios as the total sample. Resonances in the range 5.1–5.3 p.p.m. (Fig. 1b) assigned to H-1 of the arabinan seem to be representative of the ratios of signal intensities observed in the non-enriched material (Fig. 1a). This single precipitation step corresponded to a 10–15-fold purification of the arabinan with a recovery of ~40%. The $^1H$-n.m.r. spectrum of the copper sulphate-soluble fraction (Fig. 1b) can be used to rule out significant 2-substitution by α-arabinofuranosyl of the xylose-substituted glucose residues, as found in an oligosaccharide derived from an extracellular xyloglucan of sycamore[15]. In this oligosaccharide, the arabinosyl group caused downfield shifts (of up to 0.04 p.p.m.) of the resonances of neighbouring xylosyl residues[15]. No such shifts are observed in Fig. 1b. The $^{13}C$-n.m.r. spectrum of the copper sulphate-soluble fraction (Fig. 2c) contained signals associated with galactoxyloglucan features (Fig. 2a) and significant resonances from branched

arabinans[24,25] that had chemical shifts identical to those of the minor signals in Fig. 2b but with much increased intensity. In addition, minor resonances that corresponded to (1→4)-β-D-galactan structures[28] were detected, *e.g.*, for C-4 at 78.8 p.p.m. A minor $^1$H signal at 4.65 p.p.m. (Fig. 1b) was assigned tentatively to H-1 of (1→4)-β-D-galactan linkages. The presence of both arabinan and galactan in tamarind-seed polysaccharides suggests that a small amount of pectic material was co-extracted with the preponderant galactoxyloglucan. Although the present results suggest that arabinans are not present as free oligomers or as short side chains attached to the galactoxyloglucan backbone, it has not been established whether covalent linkages connect the two species.

*Solution properties.* — (*a*) *Small-angle X-ray scattering.* The data were recorded over the angular range $2\Theta = 0.2$–$4.9°$, which corresponded to scattering vectors ($h$) of $1.5 \times 10^{-2}$–$3.5 \times 10^{-1}$ Å$^{-1}$ ($h = 4\pi \sin \Theta/\lambda$). Typical data for a 1% (w/w) solution of purified tamarind-seed polysaccharide are shown in Fig. 3a; for appropriate ranges of $h$, a plot of ln (intensity × $2\Theta$) versus $h^2$ contained a linear (cross-sectional Guinier)

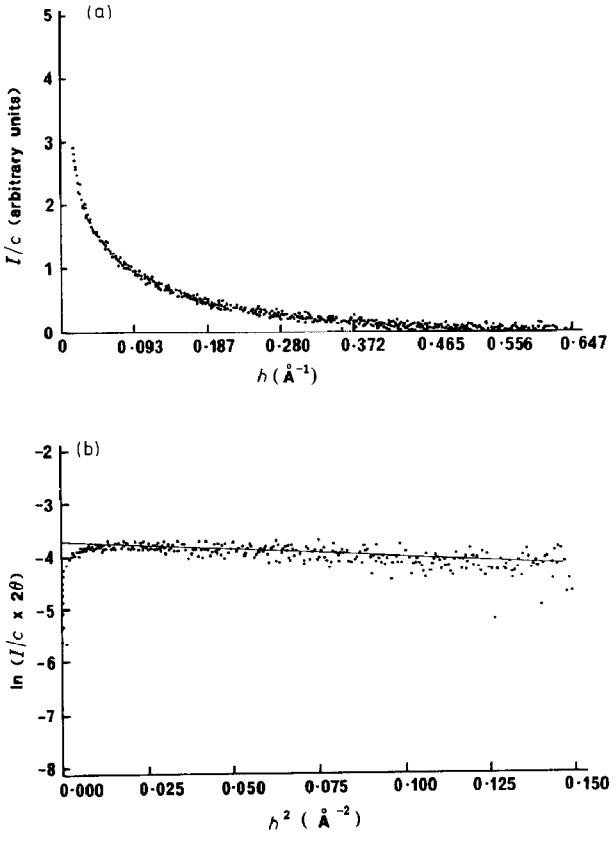


Fig. 3. (*a*) Angular dependence of the small-angle X-ray scattering intensity from an aqueous solution (10 mg/mL) of tamarind-seed polysaccharide; (*b*) cross-sectional plot of the scatter curve (*a*) from an aqueous solution (10 mg/mL) of tamarind-seed polysaccharide. The slope of the fitted straight line corresponds to $R_c$ = 2.8 Å.

region, the slope of which was proportional to $R_c^2$, where $R_c$ is the cross-sectional radius of gyration[29]. Such a plot is shown in Fig. 3b for the data of Fig. 3a, and the linear region is seen for $0.02 < h^2 < 0.15$ Å$^{-2}$, the slope of which corresponded to $R_c = 2.8$ Å. Measurements were made for 12 solutions of tamarind-seed polysaccharide in the range 0.5–2.5% (w/w), and $R_c$ values in the range 2.6–3.2 Å were obtained with an average value of 2.9 ±0.2 Å. This value may be compared with values of 2.0 Å for linear dextran[30], 2.5 ±0.8 Å and 2.6 ±0.8 Å for iota-carrageenan[31] and agarose[32], 2.6 ±0.7 Å for guar galactomannan[33], and 3.0 Å for hyaluronic acid[34]. For each of these systems, the $R_c$ value corresponded to single chains in solution and this applies also to the tamarind-seed polysaccharide, the $R_c$ value of 2.9 Å being at the top end of the range, presumably due to the high degree of substitution by side chains.

The derived $R_c$ value, however, is an average and the X-ray data alone cannot rule out a limited amount of aggregation of chains. The conclusion from Fig. 3, therefore, is that tamarind-seed polysaccharide in solution at 25° is in a substantially disaggregated state of single chains.

(*b*) *Light scattering*. Static light-scattering experiments on solutions can yield the weight-average molecular weight ($M_w$), the root-mean-square radius of gyration ($R_g = <S^2>^{1/2}$), and the second virial coefficient, $A_2$. Further information can be obtained from quasi-elastic or dynamic experiments; on extrapolation of the apparent diffusion coefficients to zero angle and concentration in a "dynamic" Zimm plot[35], the intercept gives the translational diffusion coefficient ($D_z$) of the polymer. The diffusion coefficient can be converted into an equivalent hydrodynamic radius of a hard sphere, following the Stokes–Einstein equation.

$$<R_h> = kT/(6\pi\eta_o D_z). \qquad (1)$$

where $\eta_o$ is the viscosity of the solvent, $k$ is the Boltzmann constant, and $T$ is the temperature (K).

Since $R_h$ is the radius of a hypothetical sphere with the diffusion coefficient $D_z$, the ratio between radius of gyration and hydrodynamic radius, $\rho \equiv R_g/R_h$, is sensitive to the shape of the particle. Static and dynamic Zimm plots for aqueous solutions of purified tamarind-seed polysaccharide are presented in Figs. 4a and 4b, respectively. The data obtained from these plots together with the $\rho$-parameter and the characteristic ratio $C_\infty$ are collected in Table II.

The parameter $C_\infty$ (the characteristic ratio) is an estimate of the rigidity of the polymer and is given by

$$C_\infty = 6<S^2>M_o/(l^2 M_w). \qquad (2)$$

where $l$ is the length of one chain segment and $M_o$ is the molecular weight of this segment. If the molecule is assumed to be single-stranded and each $\beta$-(1→4)-linked glucose residue in the backbone is defined as one segment of the chain, the values $l = 0.52$ nm and $M_o = 360$ (= 162/0.45) apply[6] and result in $C_\infty = 110$. This value may be

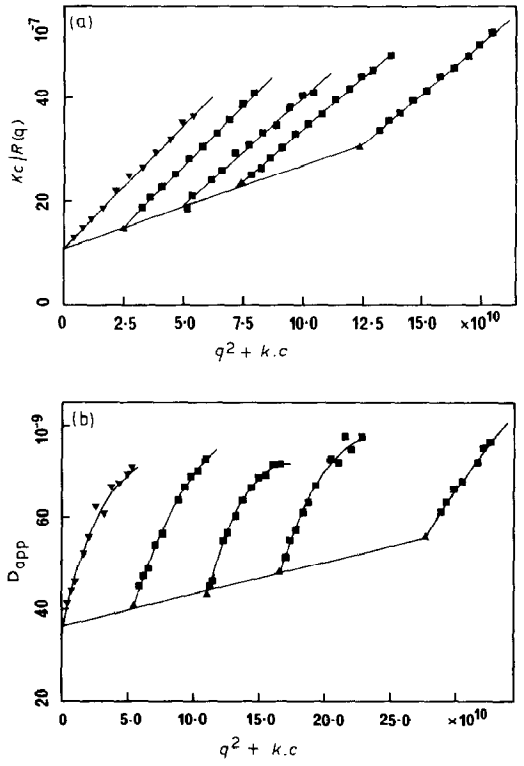


Fig. 4. (*a*) Static Zimm plot of tamarind-seed polysaccharide for aqueous solutions of (left to right) 0.0, 0.248, 0.496, 0.744, and 1.24 mg/mL; (*b*) dynamic Zimm plot of the same solutions.

compared with that for guar galactomannan and carboxymethylcellulose, which have similar backbone structures but characteristic ratios[36] that are lower by a factor of ~10. The greater stiffness of the chain of tamarind-seed polysaccharide compared to that of carboxymethylcellulose might be due partially to the high proportion of side chains in the former (~80% of glucose residues are substituted). Inspection of space-filling (CPK) molecular models suggests that the side chains (especially the disaccharide units)

TABLE II

Parameters determined from static and dynamic light-scattering measurements on aqueous solutions of tamarind-seed polysaccharide[a]

| | |
|---|---|
| $M_w$ | $8.8 \times 10^5 \pm 0.1$ g/mol. |
| $R_g$ | $110 \pm 1.0$ nm. |
| $A_2$ | $8.5 \times 10^{-4} \pm 0.5$ mol.mL/g$^2$. |
| $D_z$ | $3.4 \pm 0.2 \times 10^{-8}$ cm$^2$/s. |
| $R_h$ | $71 \pm 3.0$ nm. |
| $C_\infty$ | $110 \pm 1$. |
| $\rho$ | $1.55 \pm 0.08$. |

[a] Average values for measurements from 2 samples purified separately.

cause significant barriers to the mobility of the internal chains, particularly at high levels of substitution. The $C_\infty$ value for tamarind-seed polysaccharide is higher than those for other neutral polysaccharides[37] and is comparable to those for alginates that have a ribbon-like structure stiffened by mutual electrostatic repulsion between adjacent residues. However, it is possible that the stiffness of the chain of tamarind-seed polysaccharide is not due solely to hindered rotation but also to specific aggregation which will be discussed elsewhere[38]. Because of the marked stiffness of the chain, a $\rho$-parameter would be expected that is significantly different from the value found experimentally for flexible coils[39]. In fact, a value of $\rho$ of 1.55 lies in the range intermediate between that (1.27) for flexible, nearly monodisperse coils in a $\Theta$ solvent[40] and that (2–3) for such highly ordered polysaccharides[19,41] as gellan or xanthan. Several factors are expected to increase the value of $\rho$ above that for monodisperse coils in a $\Theta$ solvent, namely, the quality of the solvent and the drainage, polydispersity[39], and stiffness of the chain[42]. All of these factors apply to tamarind-seed polysaccharide, and their combination is presumed to be responsible for the observed increase in the value of $\rho$ to 1.55. However, this value is significantly lower than that reported for microbial polysaccharides in the helical ordered state, which have comparable virial coefficients and, probably, similar polydispersity but greater stiffness of the chains[41].

(*c*) *Rheology*. Two features of the solution rheology of tamarind-seed polysaccharide have been studied, namely, the intrinsic viscosity $[\eta]$ and the dependence of the "zero-shear" viscosity $\eta_0$ on concentration. For purified tamarind-seed polysaccharide, an average intrinsic viscosity of $[\eta] = 6 \pm 0.5$ dL/g was obtained. Knowing the radius of gyration and the molecular weight from the light-scattering experiments, an attempt can be made to predict the intrinsic viscosity from the Fox–Flory theory[43].

$$[\eta] = \Phi 6^{3/2} < S^2 >^{3/2} / M. \tag{3}$$

With a value[44] of $\Phi = 2.5 \times 10^{23}$ mol$^{-1}$, this approach yields a theoretical intrinsic viscosity of $[\eta]_{th} = 50.4$ dL/g, which is about eight times higher than the corresponding experimental value. This discrepancy may be due to polydispersity, excluded volume, and draining effects. The first two parameters influence the radius of gyration and the last alters the parameter $\Phi$.

Equation *3* is strictly valid only for mono-disperse chains, which means that the value estimated for $[\eta]_{th}$ will be too high, as the *z-average* of the radius of gyration is divided by the *weight average* of the molecular weight. On the assumption of a most probable size distribution,

$$< S^2 >_z = < 1.5 S^2 >_w, \tag{4}$$

the theoretical value from equation *3* becomes $[\eta]_{th} = 30.1$ dL/g.

The radius of gyration is influenced by the excluded volume effect, expressed by the expansion factor $\alpha_{\xi^2}$, and defined by equation *5*.

$$<S^2> = <S_o^2>\alpha_{s2} \quad (5)$$

where $<S_o>$ is the radius of gyration of the unperturbed chain. The factor $\alpha_{s2}$ may be calculated from static light-scattering results via the interpenetration function[44] $\psi(\alpha)$ given by

$$A_2 = 4\pi^{3/2}N_A<S^2>^{3/2}/M^2\psi(\alpha), \quad (6)$$

$$\text{where } \psi(\alpha) = 0.19814\{1-[1 + 0.382(1-\alpha^{-3})]^{-7.39}\}. \quad (7)$$

From equations *6* and *7*, a value for $\alpha_{s2}$ of 1.06 is calculated.

The parameter[44] $\Phi$ in equation *3* may be corrected according to the formula

$$\Phi = 2.5*10^{23}\,\alpha_{s2}{}^{-0.57}, \quad (8)$$

in order to yield a theoretical intrinsic viscosity (corrected for polydispersity) of $[\eta]_{th} = 29.15$, which suggests that the effect of excluded volume is almost negligible.

The value of $\alpha_{s2}$, obtained from the above interpenetration function, is derived from static light-scattering data and ignores drainage effects. An alternative method of estimating $\alpha_{s2}$ involves a combination of static and hydrodynamic contributions. From a wide variety of experimental data[39], the product $A_2M_w[\eta]^{-1}$ has been found to be a universal function of $\alpha_{s2}$. Using this relationship, a value for $\alpha_{s2}$ of 1.65 was found, which is significantly different from that derived above. This finding indicates that the properties in solution of the tamarind-seed polysaccharide are highly disturbed by hydrodynamic effects, *i.e.*, the effect of draining.

The draining parameter $h = X/\sqrt{2}$ may be derived in two ways. The first involves a calculation of the hypothetical parameter $\Phi_{th}$, which would predict intrinsic viscosity correctly. From this quantity, the value for $X$ can be calculated from the equation[45]

$$\Phi = (\pi/6)^{3/2}N_A[XF(X)], \quad (9)$$

where $[XF(X)]$ is the Kirkwood–Riseman viscosity function, which is calculated to be 0.2178. If $[XF(X)]$ is plotted[45] against $X$, the latter is read off graphically to be 0.344, which results in a draining parameter $h = 0.243$.

A second approach deals with data from light scattering. Thus, $h$ can be interpreted as the ratio between non-draining and draining contributions to the diffusion coefficient where the former may be calculated from the radius of gyration. For ideal non-draining random coils, a value of $\rho$ of 1.27 was found experimentally[40], which, together with the radius of gyration from Table II, yielded a hypothetical hydrodynamic radius of $R_h = 86.6$ nm. This value corresponds, via the Stokes–Einstein relation, to a diffusion coefficient $D_z\text{nd} = 2.83 \times 10^{-8}\ \text{cm}^2.\text{s}^{-1}$ for the ideal non-draining limit.

When the behaviour deviates from ideal due to drainage effects, the experimental diffusion coefficient $D_z$ex may be expressed as the sum of draining and non-draining contributions

$$h = (D_z\text{ex} - D_z\text{nd})/D_z\text{nd}, \tag{10}$$

which results in a value of $h$ of 0.219 in good agreement with the value (0.243) derived from intrinsic viscosity data. This finding suggests that drainage may be the major cause of the non-ideal $\rho$ value obtained (see the section on light scattering). Therefore, it is concluded that the drainage of the solvent through the coils of the polymer is significant in aqueous solutions of tamarind-seed polysaccharide and that this effect is responsible (together with polydispersity) for the large difference between experimental and predicted (equation *3*) intrinsic viscosities.

Information concerning the hydrodynamic behaviour of finite concentrations can be obtained conveniently from a plot of "zero-shear" specific viscosity ($\eta_{sp}$) against the product of concentration ($c$) and intrinsic viscosity ($[\eta]$). As the intrinsic viscosity value is related to the volume occupied by an isolated polymer molecule, $c[\eta]$ is a measure of the total volume occupied by polymer molecules at a particular concentration. By using a range of viscometers, extrapolated values of the "zero-shear" viscosity were obtained for aqueous solutions of tamarind-seed polysaccharide in the range 0.03–3.0% (w/v). These data are presented as a double logarithmic plot of "zero-shear" specific viscosity versus $c[\eta]$ in Fig. 5. As found previously for synthetic polymers[46,47] and disordered polysaccharides[47,48], two limiting slopes were obtained that corresponded to "dilute" and "semi-dilute" solution conditions[46]. The transition between these two states occurs when individual polymer coils begin to interpenetrate and has been represented as a single discontinuity[47] (solid line in Fig. 5) or as two discontinuities[48] (dashed line in Fig. 5) but, most probably, the transition is gradual and reflects the gradual nature of viscosity-detected coil interpenetration with increasing concentration.

For such random-coil polysaccharides as dextran, sodium alginate, lambda-carrageenan[47], and amylose[49], slopes of $\log \eta_{sp}$ *vs.* $\log c[\eta]$ in "dilute" and "semi-dilute" regimes were 1.3–1.4 and 3.3–3.4, respectively. Extrapolated break points between the two regimes were found at values of $c[\eta]$ and $\eta_{sp}$ of $\sim 4$ and $\sim 10$, respectively[47]. For tamarind-seed polysaccharide (Fig. 5), slopes of 1.13 and 4.7 were found for "dilute" and "semi-dilute" regimes, respectively, with an extrapolated break point at $c[\eta] = 3.6$ and $\eta_{sp} = 4.5$. This behaviour is close to that of guar and carob galactomannans[47], hyaluronate at low pH and high ionic strength[47], and oat (1→3,4)-$\beta$-D-glucan[50], particularly with regard to the enhanced "semi-dilute" regime slope that showed a much greater fractional increase with concentration compared with "random coil" polysaccharides. This effect has been ascribed[47,51] to "hyperentanglements" which survive longer than non-specific entanglements. Such "hyperentanglements", however, do not necessarily predict gross aggregation effects. Most notably, guar and carob galactomannans show similar viscosity/concentration behaviour, but the latter has a much greater

tendency to form stable associations. One feature which all systems capable of "hyperentanglements" show is a certain stiffness of the chains in an essentially non-ionised environment when compared with other polysaccharide coils that show classical entanglement behaviour. Therefore, it is possible that the "hyperentanglement" phenomenon of the chains is due to a tenuous alignment of neutral and stiff segments in solution.

## EXPERIMENTAL

*Purification of the polysaccharide.* — Tamarind-seed polysaccharide Glyloids 3S and 3A (Dainippon Pharmaceutical Co., Osaka, Japan) were used in most studies, and nasturtium-seed polysaccharide was prepared as described[52]. Purified polysaccharides were obtained by dissolution (0.5–1.0% w/v) in deionised water (16 h at 25° or 10 min at 80° followed by 2–3 h at 25°), centrifugation at 20,000*g* for 30 min, extensive dialysis against deionised water, and lyophilisation.

(*a*) *Composition.* Samples (5 mg) of polysaccharide were hydrolysed[53] by the 72%–4% $H_2SO_4$ method[53], and the monosaccharides in the hydrolysates were determined quantitatively by g.l.c.[54] of the derived alditol acetates[55].

(*b*) *N.m.r. spectroscopy.* The $^1H$- (200.13 MHz) and $^{13}C$-n.m.r. (50.32 MHz) spectra were recorded for solutions in $D_2O$ at 85–90° with a Bruker AM 200 spectrometer. Samples for $^1H$-n.m.r. spectroscopy were first lyophilised from solution in $D_2O$ in order to reduce interference from residual solvent protons. Spin–lattice relaxation times ($T_1$) were determined using the inversion–recovery pulse sequence (180°–$\tau$–90°–acquire). Comparative integration of signals was achieved by excision and weighing, and by using the spectrometer integration routine. Chemical shifts are referenced to external $Me_4Si$.

*Small-angle X-ray scattering analysis.* — A Kratky camera equipped with a CGR position-sensitive detector coupled to a Canberra multi-channel analyser was used. The X-ray source was a Philips 1730 sealed-tube X-ray generator operating at the copper $K_\alpha$ wavelength (1.54 Å). Samples were prepared by dissolving purified polysaccharide in deionised water at room temperature for 16 h or by neutralisation of a solution of polysaccharide in M NaOH and extensive dialysis as for light scattering (see below). Essentially identical scattering curves were obtained for the two types of sample.

*Light scattering.* — Static and dynamic light-scattering measurements were carried out simultaneously in the angular range 30–150° with the red ($\lambda$ 647.1 nm) line of a Krypton ion laser (Spectra Physics, Model Kr 2020). Details of the apparatus and data evaluation methods have been reported[56]. The refractive index increment was measured with a Brice Phoenix 60 differential refractometer at $\lambda$ 647.1 nm. A value for d$n$/d$c$ of 0.163 cm$^3$/g was found for purified tamarind-seed polysaccharide. Stock solutions for light-scattering measurements were prepared by dissolution of purified Glyloid 3S either in M NaOH (room temperature, 16 h) followed by neutralisation, and extensive dialysis, or directly in double-distilled water. From a stock solution (typically 0.15–0.3% w/v), a series of solutions (down to 0.02% w/v) were prepared by dilutions with double-distilled water. The solutions were clarified optically by filtration through 0.45-$\mu$m Millipore one-way filters, directly into light-scattering cells.

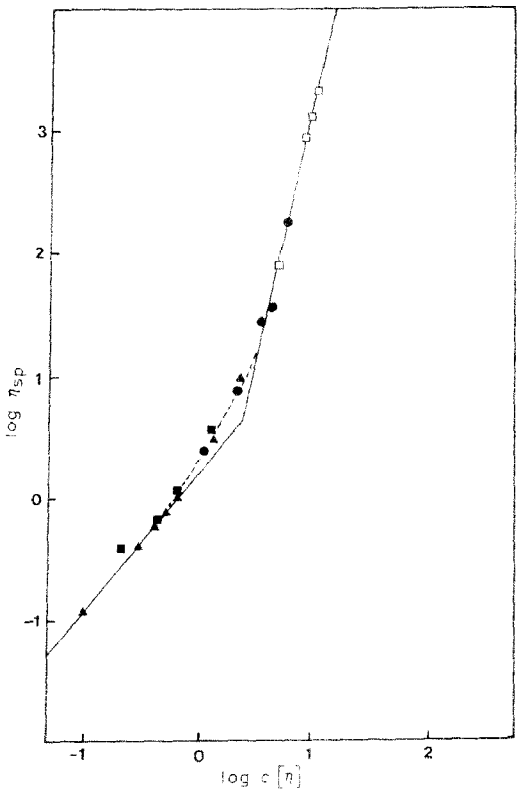


Fig. 5. Dependence of "zero-shear" specific viscosity ($\eta_{sp}$) on concentration ($c$) for aqueous solutions of tamarind-seed polysaccharide determined using an Ubelohede capillary viscometer (△), a Contraves Low Shear 30 viscometer (■), a Haake CV100 low-shear viscometer (●), or a Rheometrics Stress rheometer RSR (□).

*Rheology.* — Viscosity measurements were performed over a range of shear rates for concentrations of polysaccharide up to 3% w/v. The "zero-shear" or "Newtonian" viscosities were obtained by extrapolation. The instruments used to cover the concentration range and to validate readings between instruments for the same concentration (see Fig. 5) were capillary viscometers of the Ubelohede type (Schott Geräte, F.R.G.), a Haake low-shear viscometer type CV100, and a Contraves Low Shear 30 viscometer (Couette geometry; maximum shear rate, 1 $s^{-1}$). Values of the intrinsic viscosity were determined by standard procedures[47] from measurements on dilute solutions using the Contraves viscometer.

ACKNOWLEDGMENTS

We thank Professor W. Burchard for providing light-scattering facilities and for helpful discussions, Drs. H.-U. ter Meer and A. H. Clark for helpful comments, D. Caswell and D. Cooke for technical assistance, and the European Community for partial financial support.

REFERENCES


1 H. Meier and J. S. G. Reid, *Encycl. Plant Physiol. New Ser.*, 13A (1982) 418–471.
2 D. Reis, B. Vian, D. Darzens, and J.-C. Roland, *Planta*, 170 (1987) 60–73.
3 S. K. Hasan and S. Ijaz, *Sci. Ind.*, 9 (1972) 131–137.
4 T. Gerard, in R. L. Davidson (Ed.), *Handbook of Water-Soluble Gums and Resins*, McGraw Hill, New York, 1980, ch. 23.
5 M. Glicksman, in M. Glicksman (Ed.), *Food Hydrocolloids*, Vol. III, CRC Press, Boca Raton, Florida, 1986, pp. 191–202.
6 T. Hayashi, *Annu. Rev. Plant Physiol. Plant Mol. Biol.*, 40 (1989) 139–168.
7 P. Kooiman, *Acta Bot. Nederl.*, 9 (1960) 208–219.
8 P. Kooiman, *Recl. Trav. Chim. Pays-Bas*, 80 (1961) 849–865.
9 J. A. C. Alvarez and L. R. O. Rodriguez, *Rev. CENIC, Cienc. Fis.*, 9 (1978) 227–238.
10 J. E. Courtois and P. Le Dizet, *C. R. Acad. Sci., Ser. D*, 277 (1973) 1957–1959.
11 A. Dali-Youcef, P. Le Dizet, and J. E. Courtois, *Phytochemistry*, 18 (1979) 1949–1951.
12 E. V. White and P. S. Rao, *J. Am. Chem. Soc.*, 75 (1953) 2617–2619.
13 H. C. Srivastava and P. P. Singh, *Carbohydr. Res.*, 4 (1967) 326–342.
14 M. Mori, S. Eda, and K. Kato, *Carbohydr. Res.*, 84 (1980) 125–135.
15 L. L. Kiefer, W. S. York, P. Albersheim, and A. G. Darvill, *Carbohydr. Res.*, 197 (1990) 139–158.
16 E. R. Morris, D. A. Rees, D. Thom, and J. K. Madden, in G. O. Aspinall (Ed.), *The Polysaccharides*, Vol. 1, Academic Press, Orlando, Florida, 1982, pp. 195–290.
17 G. Paradossi and D. A. Brant, *Macromolecules*, 15 (1982) 874–879.
18 T. Sato, T. Norisuye, and H. Fujita, *Macromolecules*, 17 (1984) 2696–2700.
19 T. Coviello, K. Kajiwara, W. Burchard, M. Dentini, and V. Crescenzi, *Macromolecules*, 19 (1986) 2826–2831.
20 R. K. Richardson and S. B. Ross-Murphy, *Int. J. Biol. Macromol.*, 9 (1987) 257–264.
21 R. K. Richardson and S. B. Ross-Murphy, *Int. J. Biol. Macromol.*, 9 (1987) 250–256.
22 W. S. York, J. E. Oates, H. van Halbeek, A. G. Darvill, P. Albersheim, P. R. Tiller, and A. Dell, *Carbohydr. Res.*, 173 (1988) 113–132.
23 M. Edwards, I. C. M. Dea, P. V. Bulpin, and J. S. G. Reid, *J. Biol. Chem.*, 261 (1986) 9489–9494.
24 P. Capek, R. Toman, A. Kardosova, and J. Rosik, *Carbohydr. Res.*, 117 (1983) 133–140.
25 J.-P. Joseleau, G. Chambat, M. Vignon, and F. Barnoud, *Carbohydr. Res.*, 58 (1977) 165–175.
26 S. C. Churms, E. H. Merrifield, A. M. Stephen, D. R. Walwym, A. Polson, K. J. van der Merwe, H. S. C. Spies, and N. Costa, *Carbohydr. Res.*, 113 (1983) 339–344.
27 K. Mizutani, R. Kasai, M. Nakamura, O. Tanaka, and H. Matsuura, *Carbohydr. Res.*, 185 (1989) 27–38.
28 R. Pressey and D. S. Himmelsbach, *Carbohydr. Res.*, 127 (1984) 356–359.
29 O. Glatter and O. Kratky, *Small-Angle X-Ray Scattering*, Academic Press, London, 1982.
30 S. K. Garg and S. S. Stivala, *J. Polym. Sci., Polym. Phys. Ed.*, 16 (1978) 1419–1434.
31 A. H. Clark and C. D. Lee-Tuffnell, in J. R. Mitchell and D. R. Ledward (Eds.), *Functional Properties of Food Macromolecules*, Elsevier Applied Science, London, 1986, pp. 203–271.
32 M. Djabourov, A. H. Clark, D. W. Rowlands, and S. B. Ross-Murphy, *Macromolecules*, 22 (1989) 180–188.
33 D. W. Rowlands, unpublished observations.
34 R. L. Cleland, *Arch. Biochem. Biophys.*, 180 (1977) 57–68.
35 W. Burchard, *Makromol. Chem., Macromol. Symp.*, 18 (1988) 1–35.
36 G. Robinson, S. B. Ross-Murphy, and E. R. Morris, *Carbohydr. Res.*, 107 (1982) 17–32.
37 E. R. Morris, D. A. Rees, E. J. Welsh, L. G. Dunfield, and S. G. Whittington, *J. Chem. Soc., Perkin Trans. 2*, (1978) 793–800.
38 M. Dentini, P. Lang, V. Crescenzi, and W. Burchard, unpublished data.
39 W. Burchard, *Adv. Polym. Sci.*, 43 (1983) 1–124.
40 M. Schmidt and W. Burchard, *Macromolecules*, 14 (1981) 210–211.
41 M. Dentini, T. Coviello, W. Burchard, and V. Crescenzi, *Macromolecules*, 21 (1988) 3312–3320.
42 M. Schmidt, *Macromolecules*, 17 (1983) 553–560.
43 T. G. Fox and P. J. Flory, *J. Am. Chem. Soc.*, 73 (1951) 1904–1908.
44 H. Yamakawa, *Modern Theory of Polymer Solutions*, Harper and Row, New York, 1971.
45 M. Kurata and H. Yamakawa, *J. Chem. Phys.*, 29 (1958) 311–325.
46 W. W. Graessley, *Adv. Polym. Sci.*, 16 (1974) 1–179.

47 E. R. Morris, A. N. Cutler, S. B. Ross-Murphy, D. A. Rees, and J. Price, *Carbohydr. Polym.*, 1 (1981) 5–21.
48 B. Launay, J. L. Doublier, and J. Lefebvre, in *Functional Properties of Food Macromolecules*, Elsevier, London, 1986, pp. 1–78.
49 M. J. Gidley, *Macromolecules*, 22 (1989) 351–358.
50 J. L. Doublier and G. Llamas, *Int. Symp. Cereal Carbohydrates*, Edinburgh, 1988, Abstr. 32.
51 J. D. Ferry, W. C. Child, Jr., R. Zand, D. M. Stern, M. L. Williams, and R. F. Landel, *J. Colloid Sci.*, 12 (1957) 53–67.
52 M. Edwards, I. C. M. Dea, P. V. Bulpin, and J. S. G. Reid, *Planta*, 163 (1985) 133–140.
53 J. F. Saeman, J. L. Buhl, and E. E. Harris, *Ind. Eng. Chem., Anal. Ed.*, 17 (1945) 35–37.
54 L. A. Crawshaw and J. S. G. Reid, *Planta*, 160 (1984) 449–454.
55 P. Albersheim, D. T. Nevins, P. D. English, and A. Karr, *Carbohydr. Res.*, 5 (1967) 340–345.
56 S. Bantle, M. Schmidt, and W. Burchard, *Macromolecules*, 15 (1982) 1604–1609.